Journal of Hazardous Materials 173 (2010) 194–199

Contents lists available at ScienceDirect

Journal of Hazardous Materials

journal homepage: www.elsevier.com/locate/jhazmat

CTAB-assisted synthesis of monoclinic $BiVO_4$ photocatalyst and its highly efficient degradation of organic dye under visible-light irradiation

Wenzong Yin, Wenzhong Wang*, Lin Zhou, Songmei Sun, Ling Zhang

State Key Laboratory of High Performance Ceramics and Superfine Microstructure, Shanghai Institute of Ceramics, Chinese Academy of Sciences, 1295 Dingxi Road, Shanghai 200050, PR China

ARTICLE INFO

Article history:
Received 11 March 2009
Received in revised form 11 August 2009
Accepted 16 August 2009
Available online 22 August 2009

Keywords:
Monoclinic $BiVO_4$
Photocatalyst
CTAB
De-ethylation
Conjugated chromophore structure

ABSTRACT

A highly efficient monoclinic $BiVO_4$ photocatalyst (C-BVO) was synthesized by an aqueous method with the assistance of cetyltrimethylammonium bromide (CTAB). The structure, morphology and photophysical properties of the C-BVO were characterized by XRD, FE-SEM and diffuse reflectance spectroscopy, respectively. The photocatalytic efficiencies were evaluated by the degradation of rhodamine B (RhB) under visible-light irradiation, revealing that the degradation rate over the C-BVO was much higher than that over the reference $BiVO_4$ prepared by aqueous method and over the one prepared by solid-state reaction. The efficiency of de-ethylation and that of the cleavage of conjugated chromophore structure were investigated, respectively. The chemical oxygen demand (COD) values of the RhB were measured after the photocatalytic degradation over the C-BVO and demonstrated a 53% decrease in COD. The effects of CTAB on the synthesis of C-BVO were investigated, which revealed that CTAB not only changed the reaction process via the formation of BiOBr as an intermediate, but also facilitated the transition from BiOBr to $BiVO_4$. Comparison experiments were carried out and showed that the existence of impurity level makes significant contribution to the high photocatalytic efficiency of the C-BVO.

1. Introduction

Organic dyes in textile and other industrial effluents have become one type of the major environmental contaminants. As many dyes are highly water-soluble, traditional treatment methods including flocculation, activated carbon adsorption, and biological treatment do not work efficiently [1]. Recently, photocatalysis method has played an important role in the degradation of organic dyes in wastewater [2,3]. Compared with other treatment, photocatalytic degradation has several advantages, such as the use of environmentally friendly oxidant O_2, complete mineralization, no waste disposal problem, and a necessity of only mild temperature and pressure conditions [3,4]. Moreover, the photocatalytic degradation is able to work out even at a much low concentration of organic dyes. Therefore, photocatalytic degradation is a promising solution to organic dyes. Early studies on photocatalysts mainly focused on the Ultraviolet-driven TiO_2 photocatalyst [5–7]. However, UV light takes up only *ca.* 4% of the solar energy while visible-light *ca.* 43%. Hereby, visible-light-driven photocatalysts have been the new focus [8–10].

Since $BiVO_4$ was found to be an active photocatalyst for O_2 evolution from aqueous $AgNO_3$ solution under visible-light irradiation [11], more and more attention has been attracted to the synthesis of visible-light-driven $BiVO_4$ photocatalyst. Among the three crystalline phases of $BiVO_4$, tetragonal zircon (z-t), tetragonal scheelite (s-t) and monoclinic scheelite (s-m) structures [12], it is found that the monoclinic scheelite $BiVO_4$ (*m*-$BiVO_4$) exhibits much higher photocatalytic activity than the other two tetragonal phases [13,14]. Therefore, many methods have been employed for the synthesis of *m*-$BiVO_4$, such as solid-state reaction [15,16], hydrothermal or solvothermal method [17–21], aqueous method [22–24], ultrasound- or microwave-assisted route [25,26], metal-organic decomposition [27,28], flame spray pyrolysis [29], and solution combustion method [30]. Compared with other methods, aqueous method provides a milder environment for the synthesis of monoclinic $BiVO_4$ and the reaction parameters as well as the properties of the products could be easily tuned. To the best of our knowledge, however, the synthesis of $BiVO_4$ by aqueous method with the assistance of CTAB has not been reported.

In the present study, highly efficient *m*-$BiVO_4$ photocatalyst was synthesized by a CTAB-assisted aqueous method and rhodamine B (RhB) was used as a model dye to evaluate its photocatalytic efficiency under visible-light irradiation. Furthermore, the efficiencies both in de-ethylation and cleavage of chromophore structure were investigated, respectively. The 53% decrease of the COD values for the RhB solutions after the irradiation confirmed the photocatalytic degradation of RhB. The effects of CTAB addition on the products

* Corresponding author. Tel.: +86 21 5241 5295; fax: +86 21 5241 3122.
E-mail address: wzwang@mail.sic.ac.cn (W. Wang).

0304-3894/$ – see front matter © 2009 Elsevier B.V. All rights reserved.
doi:10.1016/j.jhazmat.2009.08.068

Table 1
List of the samples prepared in different conditions.

	C-BVO	C-BVO-cal	NC-BVO	SSR-BVO	AM-BVO
CTAB	Y	Y	N	Ref. [15]	Ref. [8], [23]
Calcination	N	Y	N		

were investigated. Possible reasons for the enhanced efficiencies of *m*-$BiVO_4$ photocatalyst were discussed.

2. Experimental

2.1. Synthesis

All the reagents were of analytical purity from Shanghai Chemical Company and used without further purification. In a typical procedure, 2 mmol of NH_4VO_3 was first dissolved into 20 mL of de-ionized water at 96 °C and then the solution was cooled to room temperature. The NH_4VO_3 solution was added dropwise into a 250 mL flask containing 40 mL of CTAB solution (0.05 M) in an oil bath at 60 °C. Afterwards, 2 mmol of $Bi(NO_3)_3{\cdot}5H_2O$ was added into 20 mL of de-ionized water and stirred for about 10 min to form a hydrolyzed white floccule. The floccule suspension was added dropwise into the flask at 60 °C under stirring. After that, the flask was connected with a condenser and heated in oil bath at 80 °C for 12 h. The final product was centrifuged, washed with de-ionized water and absolute ethanol for several times, and dried in air. The as-prepared *m*-$BiVO_4$ crystals were denoted as C-BVO. For comparison, *m*-$BiVO_4$ crystals were also synthesized by solid-state reaction (SSR-BVO) according to Ref. [15] and by aqueous method (AM-BVO) as reported in Ref. [8] and [23]. The major samples prepared in our experiment were denoted and listed in Table 1.

2.2. Characterization

The X-ray diffraction (XRD) patterns of the samples were measured with a Rigaku D/Max-2200PC diffractometer using monochromatized Cu Kα radiation (λ = 0.15418 nm) at a scanning rate of 8°/min. The field emission scanning electron microscope (FE-SEM) images were obtained on a JEOL JSM-6700F field emission scanning electron microscope. The diffuse reflectance spectra (DRS) of the $BiVO_4$ samples and the UV–vis absorption spectra of the RhB solutions were obtained on a Hitachi U-3010 UV–vis spectrophotometer.

2.3. Photocatalytic efficiency

RhB shows a major absorption band centered at 553 nm which is used to monitor the photocatalytic degradation of RhB. The photocatalytic efficiencies of the $BiVO_4$ were evaluated by the degradation of RhB under visible-light irradiation. The visible-light irradiation was provided by a 500 W Xenon lamp (Shanghai Yaming Lighting Co. Ltd.) with a 420 nm cutoff filter. Each experiment was performed at room temperature as follows: 0.1 g of $BiVO_4$ photocatalyst was added into 100 mL of RhB solution with a concentration of 10^{-5} M. Before illumination, the suspension was stirred in the dark for 12 h to ensure adsorption/desorption equilibrium between RhB and the photocatalyst. Then the suspension was stirred and exposed to visible-light irradiation. At given time intervals, 2 mL of the suspensions was taken out and centrifuged to remove the photocatalyst particles. The concentrations of the centrifuged RhB solutions were monitored using a Hitachi U-3010 UV–vis spectrophotometer. Chemical oxygen demand (COD) measurements were carried out by the dichromate titration method [31] on the RhB solutions before and after 8 h of visible-light irradiation over 0.2 g of the C-BVO. The initial concentration of the RhB solution is 2×10^{-4} M.

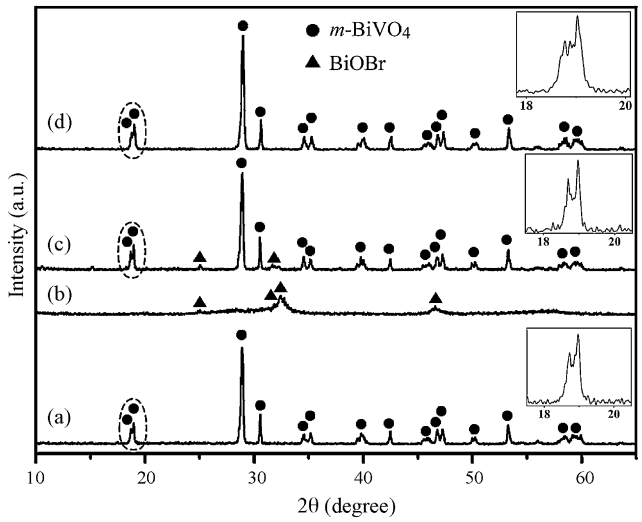

Fig. 1. XRD patterns of the C-BVO (a), the products prepared by CTAB-assisted aqueous method at 80 °C for 3 h (b) and 6 h (c), and the C-BVO-cal (d). Inset: the widened parts of XRD patterns near 19°, showing the characteristic split of monoclinic $BiVO_4$.

3. Results and discussion

3.1. Characterization of the C-BVO

Fig. 1a shows the XRD pattern of the C-BVO. All the diffraction peaks can be indexed to *m*-$BiVO_4$ which is identical to the standard (JCPDS no. 14-0688). Characteristic splitting of peaks at 18.5°, 35°, and 46° of 2θ is observed for *m*-$BiVO_4$. The sharp and narrow diffraction peaks indicate a high crystallinity of the *m*-$BiVO_4$. No diffraction peaks of other phases are detected.

Fig. 2 shows the SEM images of the C-BVO. The shapes of the C-BVO particles are nearly spherical. The sizes of these particles range from 400 nm to 700 nm. Magnified image in Fig. 2b shows a rough surface of the C-BVO particles.

The diffuse reflectance spectrum (DRS) of the C-BVO is shown in Fig. 3a. It is obvious that the absorption edge of the DRS curve possesses an elongated tail, which suggests the formation of surface states and impurity levels [13].

3.2. Photocatalytic efficiency of the C-BVO

The characteristic absorption of RhB which lies at the wavelength of 553 nm has been used to monitor the photocatalytic degradation process. Fig. 4 represents the decrease of RhB (C/C_0) as a function of irradiation time without photocatalyst and over the C-BVO, AM-BVO and SSR-BVO. Here, C is the absorption of RhB at the wavelength of 553 nm and C_0 is the absorption of RhB after the adsorption equilibrium on $BiVO_4$ photocatalysts before irradiation. The photolysis of RhB under visible-light irradiation is neglectable (Fig. 4d), as reported in Ref. [17]. RhB is almost completely degraded after 20 min of irradiation over the C-BVO under visible-light (Fig. 4a). However, only about 12.5% of RhB can be degraded over the SSR-BVO and 85% over the AM-BVO after 120 min of irradiation (Fig. 4b and c). According to Ref. [32], the RhB degradation over the photocatalysts is fitted for pseudo-first-order kinetics and the reaction constant k, which was used to evaluate the degradation rate, could be determined by the plots of $\ln(C/C_0)$ vs irradiation time (t). The determined k values for the C-BVO, AM-BVO and SSR-BVO are 0.233(±0.008), 1.805(±0.079) × 10^{-2}, and 8.268(±0.113) × 10^{-4} min^{-1}, respectively. Their linearly dependent coefficients (R) are 0.998, 0.996 and 1.000, respectively, indicating a good linear dependence relation. It is clear that the k value for the C-BVO is about 12 times higher than that for the AM-

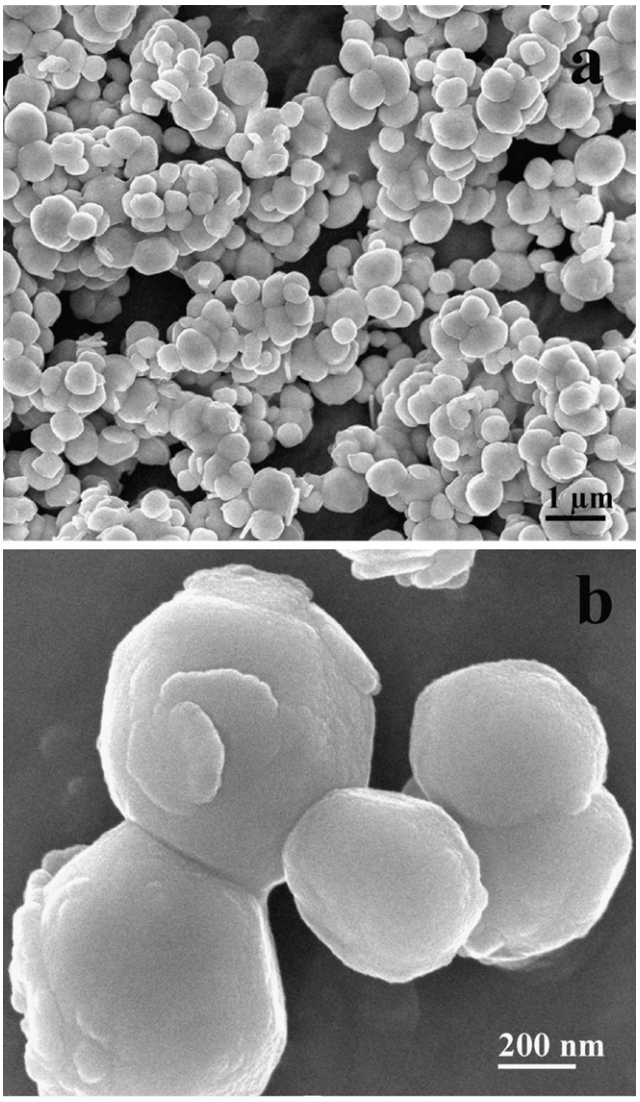

Fig. 2. SEM images of the C-BVO. (a) panoramic view; (b) magnified view.

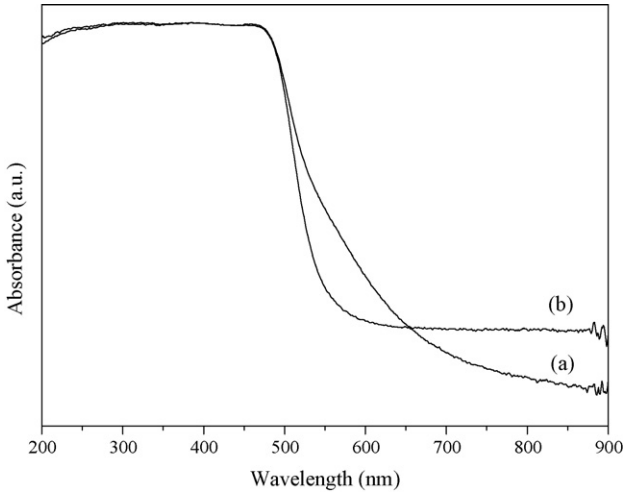

Fig. 3. DRS spectra of the C-BVO (a) and C-BVO-cal (b).

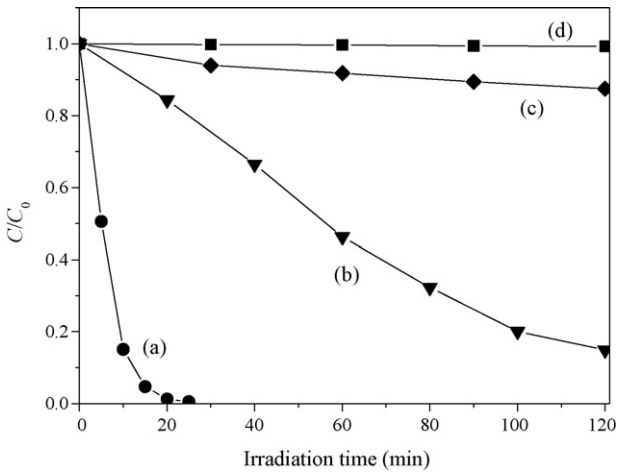

Fig. 4. Decrease of RhB (C/C_0) (100 mL, 10^{-5} M) as a function of irradiation time over 0.1 g of (a) C-BVO, (b) AM-BVO and (c) SSR-BVO, and (d) direct photolysis of RhB (100 mL, 10^{-5} M) under visible-light ($\lambda > 420$ nm).

BVO and 281 times higher than that for the SSR-BVO, indicating a high photocatalytic efficiency of the C-BVO.

As reported by Zhao et al. [33], two procedures are involved in the degradation of RhB: the de-ethylation and the cleavage of conjugated chromophore structure. The former one could be characterized by the shift of the maximum absorption band (λ_{max}) of RhB while the latter one by the change in the absorption maximum (A_{max}/A^0_{max}) of RhB. Usually these two procedures take place simultaneously in the presence of photocatalyst under irradiation. As a result, it is a cooperative effect that results in the decrease of absorbance at the wavelength of 553 nm with the irradiation time prolonged.

To investigate the efficiencies of the de-ethylation and the cleavage of conjugated chromophore structure, here we analyzed the changes in the maximum absorption bands and the absorption maxima of the RhB solutions irradiated for different time. The results are shown in Fig. 5. The C-BVO exhibits high photocatalytic efficiencies in both the de-ethylation and the cleavage of conjugated chromophore structure of RhB. During the first 20 min the de-ethylation proceeds in a stepwise manner with the color of the suspension changing from initial red to light green-yellow, as reported in the Ref. [32]. De-ethylation of the fully *N*, *N*, *N*′, *N*′-tetraethylated rhodamine molecule (RhB) results in significant hypsochromic shifts. The maximum absorption band of RhB is

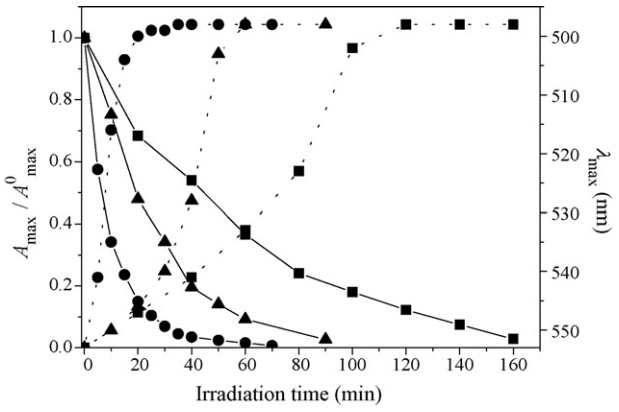

Fig. 5. Changes of the maximum absorption band (λ_{max}, dot line) and the absorption maximum (A_{max}/A^0_{max}, solid line) of RhB as a function of irradiation time during the photocatalytic degradation of RhB (100 mL, 10^{-5} M) over the C-BVO (0.1 g, circle), NC-BVO (0.1 g, square) and C-BVO-cal (0.1 g, triangle).

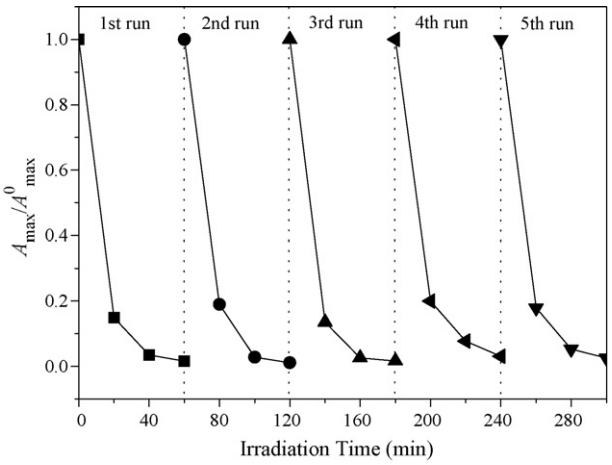

Fig. 6. Cycling runs in photocatalytic degradation of RhB (100 mL, 10^{-5} M) in the presence of the C-BVO (0.1 g) under visible-light irradiation.

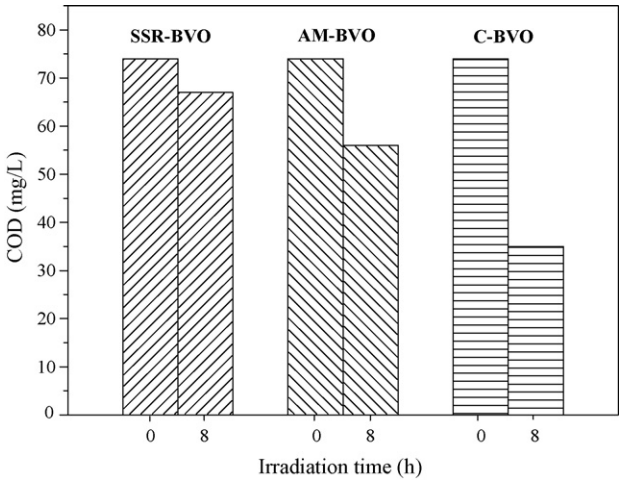

Fig. 7. Chemical oxygen demand (COD) data for the RhB solutions (100 mL, 2×10^{-4} M) before and after 8 h of irradiation over 0.2 g of the SSR-BVO, AM-BVO and C-BVO.

553 nm; of *N*, *N*, *N*′-triethylated rhodamine (TER), 539 nm; of *N*, *N*′-diethylated rhodamine (DER), 522 nm; of *N*-ethylated rhodamine (MER), 510 nm; and of rhodamine, 498 nm [34]. After 20 min of irradiation, although the absorbance at the wavelength of 553 nm decreases to zero, the maximum absorption band shifts to 500 nm and the absorption maximum decreases to 0.15, suggesting the existence of rhodamine and other rhodamine species mentioned above. After 35 min of irradiation, the maximum absorption band shifts to 498 nm while the absorption maximum remains 0.045, revealing the completion of the de-ethylation process rather than the cleavage of conjugated chromophore structure. Thereafter, the maximum absorption band remains while the absorption maximum continues to decrease and reaches zero after 70 min of irradiation, indicating the complete degradation of rhodamine.

The stability of the highly efficient C-BVO photocatalyst was evaluated by recycled runs in the photocatalytic degradation of RhB under visible-light irradiation ($\lambda > 420$ nm). The decreases of the absorption maximum of RhB are shown in Fig. 6. It is clear that photocatalytic efficiency does not exhibit significant loss after five recycles, indicating that the C-BVO has high stability and does not suffer from photocorrosion during the photocatalytic degradation of RhB.

As is known, chemical oxygen demand (COD) value reflects the general concentration of organics in solution and has been widely used to evaluate the degree of degradation or mineralization of organic species during irradiation period [35]. The COD values of the RhB solutions before and after 8 h of irradiation over the SSR-BVO, AM-BVO and C-BVO were measured and the results are represented in Fig. 7. The initial COD concentration of the RhB solution (100 mL, 2×10^{-4} M) is 74 mg/L. After 8 h of irradiation under visible-light, the COD concentration of the RhB solution over the C-BVO decreases *ca.* 53% to 35 mg/L. This is significantly lower than that over the SSR-BVO (67 mg/L) and over the AM-BVO (56 mg/L), confirming the higher photocatalytic degradation rate of the C-BVO under visible-light.

3.3. Effects of CTAB on the $BiVO_4$ crystals and the photocatalytic efficiency

To investigate the effects of CTAB on the product and the photocatalytic efficiency, $BiVO_4$ crystals were also synthesized by a non-CTAB aqueous method at 80 °C for 12 h (denoted as NC-BVO) and 24 h under otherwise identical conditions. The XRD patterns of the products are shown in Fig. 8. There are two crystalline phases of $BiVO_4$ in NC-BVO: the *m*-$BiVO_4$ as mentioned above and the $BiVO_4$ (z-t) crystals (JCPDS no. 14-0133) (Fig. 8a). Even when the temperature is held for 24 h, the $BiVO_4$ (z-t) crystals still exist (Fig. 8b). However, the intensity of the diffraction peaks decreases significantly and some diffraction peaks even disappear, which might be attributed to the phase transition from $BiVO_4$ (z-t) to *m*-$BiVO_4$ [22]. It was reported that the $BiVO_4$ (z-t) crystals, with the band gap energy of 2.9 eV, possessed an ultraviolet absorption band [13]. As a result, the existence of $BiVO_4$ (z-t) phase other than *m*-$BiVO_4$ phase will decrease the photocatalytic efficiency of the NC-BVO, which was confirmed by the photocatalytic degradation of RhB over the NC-BVO (Fig. 5). It can be seen that the maximum absorption band does not shift to 498 nm until 120 min of irradiation and the absorption maximum decreases to 0.03 rather than zero even after 160 min of irradiation, indicating the drop of photocatalytic efficiencies in both the de-ethylation and the cleavage of conjugated chromophore structure.

For further investigation, the intermediate, which appeared in the synthesis of *m*-$BiVO_4$ photocatalyst by the CTAB-assisted aqueous method, was identified by XRD. The results are shown in Fig. 1. When the temperature is held at 80 °C for 3 h, only BiOBr (JCPDS no.

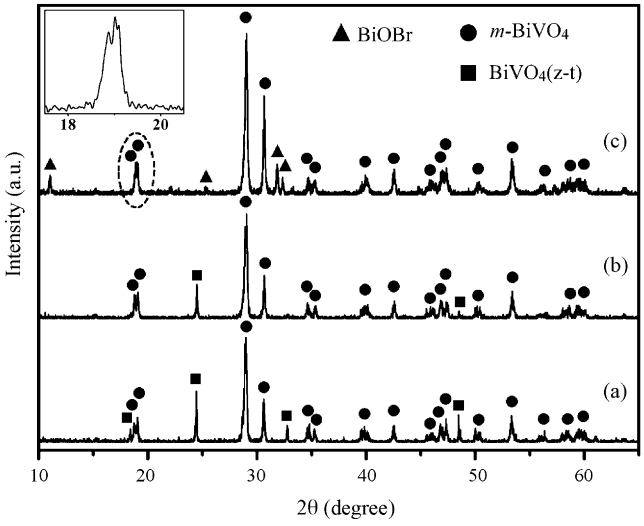

Fig. 8. XRD patterns of the NC-BVO (a), and the $BiVO_4$ crystals prepared by aqueous method at 80 °C for 24 h without CTAB (b) and for 12 h with NaBr instead of CTAB (c). Inset: magnified image of the diffraction peak near 19° in pattern (c), showing the characteristic split of monoclinic $BiVO_4$.

09-0393) is obtained (Fig. 1b). As the holding time increases from 3 h to 6 h, the intensities of the diffraction peaks corresponding to BiOBr decrease while the peaks corresponding to *m*-$BiVO_4$ emerge (Fig. 1c). When the holding time is prolonged to 12 h, the diffraction peaks of BiOBr can not be found. Instead, there are only diffraction peaks of *m*-$BiVO_4$ crystal in the XRD pattern (Fig. 1a).

The above analysis reveals that CTAB has changed the reaction process for the synthesis of *m*-$BiVO_4$. When CTAB is not introduced into the aqueous solution, $BiVO_4$ (z-t) and *m*-$BiVO_4$ are produced simultaneously and the $BiVO_4$ (z-t) gradually transforms into *m*-$BiVO_4$ with the time prolonged. Relevant chemical reactions can be formulated as follows:

$$Bi(NO_3)_3 + H_2O \rightarrow BiONO_3 + 2H^+ + 2NO_3^- \quad (1)$$

$$BiONO_3 + VO_3^- \rightarrow BiVO_4(z\text{-}t) + NO_3^- \quad (2\text{-}1)$$

$$BiONO_3 + VO_3^- \rightarrow m\text{-}BiVO_4 + NO_3^- \quad (2\text{-}2)$$

$$BiVO_4(z\text{-}t) \rightarrow m\text{-}BiVO_4 \quad (3)$$

When suitable quantity of CTAB is added into the solution, the reactions take place in a different way:

$$Bi(NO_3)_3 + H_2O \rightarrow BiONO_3 + 2H^+ + 2NO_3^- \quad (4)$$

$$BiONO_3 + Br^- \rightarrow BiOBr + NO_3^- \quad (5)$$

$$BiOBr + VO_3^- \rightarrow m\text{-}BiVO_4 + Br^- \quad (6)$$

In this process, *m*-$BiVO_4$ is produced with the BiOBr as an intermediate. As a result, pure *m*-$BiVO_4$ can be prepared by the aqueous method at 80 °C for 12 h with the assistance of CTAB.

It has been reported that the polar groups ionized from surfactant could interact with ions of opposite charge due to the electrostatic force and form an active center to accelerate the nucleation of crystals [36]. To investigate it in detail, NaBr, instead of CTAB, was used as the Br^- source to assist the synthesis of *m*-$BiVO_4$ crystals by the aqueous method at 80 °C for 12 h. The XRD pattern of the product is shown in Fig. 8c. It is clear that there are diffraction peaks of BiOBr in addition to that of *m*-$BiVO_4$, suggesting the incompletion of reaction (6). However, when CTAB rather than NaBr is involved in the synthesis, the CTA^+, which is ionized from CTAB, can bond with VO_3^- and accelerate the transition from BiOBr to *m*-$BiVO_4$. As a result, reaction (6) could complete when the aqueous solution is held at 80 °C for 12 h.

3.4. Reasons for the enhanced efficiency of the C-BVO photocatalyst

The photocatalytic efficiencies of $BiVO_4$ crystals are influenced by many factors, such as the crystal phase, size, crystallinity, surface area, bond distortion, impurity level etc. When it comes to the C-BVO crystals, the crystal phase should be an important factor that enhances the photocatalytic efficiency. The BET surface areas of the C-BVO, AM-BVO and SSR-BVO were measured to be 1.75 $m^2\,g^{-1}$, 3.13 $m^2\,g^{-1}$ and 0.26 $m^2\,g^{-1}$, respectively. As the C-BVO does not show the largest surface area, it is reasonable to speculate that the BET surface area does not play a leading role for the highest photocatalytic efficiency of the C-BVO. Another factor may be the existence of impurity level which could bring about the shift of absorption edge to the long wavelength side by narrowing the band gap of the C-BVO photocatalyst and thus expand the wave band that the C-BVO could respond [37].

To further test the above proposition, the C-BVO was calcined at 500 °C for 3 h to eliminate the impurity level (denoted as C-BVO-cal). The XRD patterns of the C-BVO and C-BVO-cal (Fig. 1c and d) reveal that the C-BVO-cal has the same *m*-$BiVO_4$ phase as the C-BVO. The BET surface area of the C-BVO-cal was measured to be 0.84 $m^2\,g^{-1}$. This is much smaller than that of the C-BVO, which could respond for the decline of photocatalytic efficiency of the C-BVO-cal. Diffuse reflectance spectrum of the C-BVO-cal in Fig. 3b shows that the prolonged tail of the absorption edge of the C-BVO crystals has disappeared after calcination. This indicates that the impurity level in the C-BVO crystals is removed through calcination. Photocatalytic efficiency of the C-BVO-cal was also evaluated by the degradation of RhB under visible-light irradiation with other experimental conditions unchanged. The result is presented in Fig. 5. It can be seen that after 60 min of irradiation the maximum absorption band shifts from 553 nm to 498 nm and the absorption maximum decreases by *ca.* 91–0.09%. It is obvious that the photocatalytic efficiency decreases significantly after the elimination of impurity level by calcination. However, the origin of the impurity level is to be investigated.

4. Conclusions

Monoclinic $BiVO_4$ crystals with the size ranging from 400 nm to 700 nm were synthesized by a CTAB-assisted aqueous method. The given RhB solution (100 mL, 10^{-5} M) was degraded in 20 min over the C-BVO photocatalyst under visible-light irradiation, which was much higher than that over the AM-BVO and over the SSR-BVO. Moreover, the de-ethylation was completed in 35 min and the cleavage of conjugated chromophore structure in 70 min. Photocatalytic degradation of RhB (100 mL, 2×10^{-4} M) over the C-BVO also brought about a 53% decrease in COD after 8 h of irradiation under visible-light. The addition of CTAB could not only change the reaction process for the synthesis of *m*-$BiVO_4$ through the formation of BiOBr as an intermediate, but also accelerate the transition from BiOBr to *m*-$BiVO_4$. Impurity levels existed in the C-BVO crystals expanded the wave band that the C-BVO could respond and thus enhanced the photocatalytic efficiency remarkably.

Acknowledgements

This work was funded by the National Basic Research Program of China (973 Program, 2007CB613305), the National Natural Science Foundation of China (No. 50732004, 50672117) and Nanotechnology Programs of Science and Technology Commission of Shanghai (0852nm00500). We also thank Dr. Haolan Xu for his valuable discussions.

References

[1] T.Y. Zhang, T. Oyama, A. Aoshima, H. Hidaka, J.C. Zhao, N. Serpone, Photooxidative N-demethylation of methylene blue in aqueous TiO_2 dispersions under UV irradiation, J. Photochem. Photobiol. A: Chem. 140 (2001) 163–172.
[2] B. Neppolian, H.C. Choi, S. Sakthivel, B. Arabindoo, V. Murugesan, Solar/UV-induced photocatalytic degradation of three commercial textile dyes, J. Hazard. Mater. 89 (2002) 303–317.
[3] D.S. Bhatkhande, V.G. Pangarkar, A.A.C.M. Beenackers, Photocatalytic degradation for environmental applications, J. Chem. Technol. Biotechnol. 77 (2002) 102–116.
[4] W.H. Ma, J. Li, X. Tao, J. He, Y.M. Xu, J.C. Yu, J.C. Zhao, Efficient degradation of organic pollutants by using dioxygen activated by resin-exchanged Iron(II) bipyridine under visible irradiation, Angew. Chem. Int. Ed. 42 (2003) 1029–1032.
[5] M.R. Hoffmann, S.T. Martin, W. Choi, D.W. Bahnemann, Environmental applications of semiconductor photocatalysis, Chem. Rev. 95 (1995) 69–96.
[6] A.L. Linsebigler, G. Lu, J.T. Yates, Photocatalysis on TiO_2 Surfaces: Principles, Mechanisms, and Selected Results, Chem. Rev. 95 (1995) 735–758.
[7] A. Fujishima, T.N. Rao, D.A. Tryk, Titanium dioxide photocatalysis, J. Photochem. Photobiol. C: Photochem. Rev. 1 (2000) 1–21.
[8] M.C. Long, W.M. Cai, J. Cai, B.X. Zhou, X.Y. Chai, Y.H. Wu, Efficient photocatalytic degradation of phenol over Co_3O_4/$BiVO_4$ composite under visible light irradiation, J. Phys. Chem. B 110 (2006) 20211–20216.
[9] J. Tang, Z. Zou, J. Ye, Efficient Photocatalytic Decomposition of Organic Contaminants over $CaBi_2O_4$ under visible-light irradiation, Angew. Chem. Int. Ed. 43 (2004) 4463–4466.
[10] D. Chatterjee, S. Dasgupta, Visible light induced photocatalytic degradation of organic pollutants, J. Photochem. Photobiol. C: Photochem. Rev. 6 (2005) 186–205.

[11] A. Kudo, K. Ueda, H. Kato, I. Mikami, Photocatalytic O_2 evolution under visible light irradiation on $BiVO_4$ in aqueous $AgNO_3$ solution, Catal. Lett. 53 (1998) 229–230.
[12] L. Zhang, D.R. Chen, X.L. Jiao, Monoclinic structured $BiVO_4$ nanosheets: hydrothermal preparation, formation mechanism, and coloristic and photocatalytic properties, J. Phys. Chem. B 110 (2006) 2668–2673.
[13] A. Kudo, K. Omori, H. Kato, A novel aqueous process for preparation of crystal form-controlled and highly crystalline $BiVO_4$ powder from layered vanadates at room temperature and its photocatalytic and photophysical properties, J. Am. Chem. Soc. 121 (1999) 11459–11467.
[14] S. Tokunaga, H. Kato, A. Kudo, Selective preparation of monoclinic and tetragonal $BiVO_4$ with scheelite structure and their photocatalytic properties, Chem. Mater. 13 (2001) 4624–4628.
[15] M. Gotić, S. Musić, M. Ivanda, M. Šoufek, S. Popović, Synthesis and characterisation of bismuth(III) vanadate, J. Mol. Struct. 744 (2005) 535–540.
[16] W. Yao, H. Iwai, J. Ye, Effects of molybdenum substitution on the photocatalytic behavior of $BiVO_4$, Dalton Trans. (2008) 1426–1430.
[17] Y. Zhao, Y. Xie, X. Zhu, S. Yan, S.X. Wang, Surfactaut-free synthesis of hyperbranched monoclinic bismuth vanadate and its applications in photocatalysis, gas sensing, and lithium-ion batteries, Chem. Eur. J. 14 (2008) 1601–1606.
[18] J.Q. Yu, A. Kudo, Effects of structural variation on the photocatalytic performance of hydrothermally synthesized $BiVO_4$, Adv. Funct. Mater. 16 (2006) 2163–2169.
[19] X. Zhang, Z.H. Ai, F.L. Jia, L.Z. Zhang, X.X. Fan, Z.G. Zou, Selective synthesis and visible-light photocatalytic activities of $BiVO_4$ with different crystalline phases, Mater. Chem. Phys. 103 (2007) 162–167.
[20] L. Ge, Novel visible-light-driven Pt-BiVO4 photocatalyst for efficient degradation of methyl orange, J. Mol. Catal. A: Chem. 282 (2008) 62–66.
[21] L. Ren, L. Jin, J.B. Wang, F. Yang, M.Q. Qiu, Y. Yu, Template-free synthesis of $BiVO_4$ nanostructures: I. nanotubes with hexagonal cross sections by oriented attachment and their photocatalytic properties for water splitting under visible light, Nanotechnology 20 (2009) 115603.
[22] A.K. Bhattacharya, K.K. Mallick, A. Hartridge, Phase transition in $BiVO_4$, Mater. Lett. 30 (1997) 7–13.
[23] S. Kohtani, S. Makino, A. Kudo, K. Tokumura, Y. Ishigaki, T. Matsunaga, et al., Photocatalytic degradation of 4-n-nonylphenol under irradiation from solar simulator: comparison between $BiVO_4$ and TiO_2 photocatalysts, Chem. Lett. 31 (2002) 60–61.
[24] L. Zhou, W.Z. Wang, L.S. Zhang, H.L. Xu, W. Zhu, Single-crystalline $BiVO_4$ microtubes with square cross-sections: microstructure, growth mechanism, and photocatalytic property, J. Phys. Chem. C 111 (2007) 13659–13664.
[25] L. Zhou, W.Z. Wang, S.W. Liu, L.S. Zhang, H.L. Xu, W. Zhu, A sonochemical route to visible-light-driven high-activity $BiVO_4$ photocatalyst, J. Mol. Catal. A: Chem. 252 (2006) 120–124.
[26] H.M. Zhang, J.B. Liu, H. Wang, W.X. Zhang, H. Yan, Rapid microwave-assisted synthesis of phase controlled $BiVO_4$ nanocrystals and research on photocatalytic properties under visible light irradiation, J. Nanopart. Res. 10 (2008) 767–774.
[27] A. Galembeck, O.L. Alves, $BiVO_4$ thin film preparation by metalorganic decomposition, Thin Solid Films 365 (2000) 90–93.
[28] M.C. Neves, T. Trindade, Chemical bath deposition of $BiVO_4$, Thin Solid Films 406 (2002) 93–97.
[29] R. Strobel, H.J. Metz, S.E. Pratsinis, Brilliant yelllow, transparent pure, and SiO_2-coated $BiVO_4$ nanoparticles made in flames, Chem. Mater. 20 (2008) 6346–6351.
[30] H.Q. Jiang, H. Endo, H. Natori, M. Nagai, K. Kobayashi, Fabrication and photoactivities of spherical-shaped $BiVO_4$ photocatalysts through solution combustion synthesis method, J. Eur. Ceram. Soc. 28 (2008) 2955–2962.
[31] Chinese National Standard, GB 11914-89, 1989.
[32] X.F. Hu, T. Mohamood, W.H. Ma, C.C. Chen, J.C. Zhao, Oxidative decomposition of rhodamine B dye in the presence of VO_2^+ and/or Pt(IV) under visible light irradiation: N-deethylation, chromophore cleavage, and mineralization, J. Phys. Chem. B 110 (2006) 26012–26018.
[33] T. Watanabe, T. Takizawa, K. Honda, Photocatalysis through excitation of adsorbates. 1. Highly efficient N-deethylation of rhodamine B adsorbed to cadmium sulfide, J. Phys. Chem. 81 (1977) 1845–1851.
[34] C. Zhang, Y. Zhu, Synthesis of square Bi_2WO_6 nanoplates as high-activity visible-light-driven photocatalysts, Chem. Mater. 17 (2005) 3537–3545.
[35] T.X. Wu, G.M. Liu, J.C. Zhao, H. Hidaka, N. Serpone, Photoassisted degradation of dye pollutants. V. Self-photosensitized oxidative transformation of rhodamine B under visible light irradiation in aqueous TiO_2 dispersions, J. Phys. Chem. B 102 (1998) 5845–5851.
[36] L.X. Yang, Y.J. Zhu, H. Tong, W.W. Wang, Submicrotubes and highly oriented assemblies of $MnCO_3$ synthesized by ultrasound agitation method and their thermal transformation to nanoporous Mn_2O_3, Ultrason. Sonochem. 14 (2007) 259–265.
[37] R. Khan, T.J. Kim, Preparation and application of visible-light-responsive Ni-doped and SnO_2-coupled TiO_2 nanocomposite photocatalysts, J. Hazard. Mater. 163 (2009) 1179–1184.